Identification of novel ciliogenesis factors using a new *in vivo* model for mucociliary epithelial development

Julie M. Hayes, **Su Kyoung Kim**[*], **Philip B. Abitua**[*], **Tae Joo Park**, **Emily R. Herrington**, **Atsushi Kitayama**[1], **Matthew W. Grow**[2], **Naoto Ueno**[1], and **John B. Wallingford**[**]
Dept. of Molecular Cell and Developmental Biology & Institute for Cellular and Molecular Biology, University of Texas, Austin, Texas 78712

Abstract

Mucociliary epithelia are essential for homeostasis of many organs and consist of mucus-secreting goblet cells and ciliated cells. Here, we present the ciliated epidermis of *Xenopus* embryos as a facile model system for *in vivo* molecular studies of mucociliary epithelial development. Using an *in situ* hybridization-based approach, we identified numerous genes expressed differentially in mucus-secreting cells or in ciliated cells. Focusing on genes expressed in ciliated cells, we have identified new candidate ciliogenesis factors, including several not present in the current ciliome. We find that TTC25-GFP is localized to the base of cilia and to ciliary axonemes, and disruption of TTC25 function disrupts ciliogenesis. Mig12-GFP localizes very strongly to the base of cilia and confocal imaging of this construct allows for simple visualization of the planar polarity of basal bodies that underlies polarized ciliary beating. \Knockdown of Mig12 disrupts ciliogenesis. Finally, we show that ciliogenesis factors identified in the *Xenopus* epidermis are required in the midline to facilitate neural tube closure. These results provide further evidence of a requirement for cilia in neural tube morphogenesis and suggest that genes identified in the *Xenopus* epidermis play broad roles in ciliogenesis. The suites of genes identified here will provide a foundation for future studies, and may also contribute to our understanding of pathological changes in mucociliary epithelia that accompany diseases such as asthma.

INTRODUCTION

Mucociliary epithelia are critical regulators of homeostasis in many organ systems, and they generally are composed of two principle cell types, mucus-secreting goblet cells and ciliated cells. One important mucociliary epithelium is that lining the airway of vertebrates, where it acts as the first line of defense against inhaled agents. Airway goblet cells secrete mucus, which provides a physical barrier between the respiratory epithelium and the inhaled air. On the neighboring ciliated cells, dozens of large, motile cilia beat coordinately to propel the mucus to the oropharynx where it is either expectorated or swallowed (Knowles and Boucher, 2002; Raji and Naserpour, 2007; Rogers, 2003; Steinman, 1968; Toskala et al., 2005). Disruption of this mucociliary system is associated with several airway pathologies, including asthma (Knowles and Boucher, 2002; Rogers, 2003; Wanner, 1979).

[**]Author for Correspondence: wallingford@mail.utexas.edu, 1 University Station C1000, University of Texas, Austin, TX 78712, Phone: 512-232-2784, Fax: 512-471-3878.
[*]These authors contributed equally to this work.
[1]Department of Developmental Biology, National Institute for Basic Biology, Okazaki 444-8585, Japan
[2]Procella Consulting Round Rock, Texas

The initial events that underlie cell-fate specification in the mucociliary epithelia, including the vertebrate airway, remain unclear, though a recent study demonstrates a role for Sox transcription factors (Park et al., 2006b). What is more clear is that genes associated with cell fate specification are re-expressed following airway injury, including Fox- and Sox-family transcription factors and Interleukins (e.g. (Park et al., 2006a; Vermeer et al., 2003; Watkins et al., 2003). Somewhat more is known about the factors governing later differentiation of ciliated cells in the airway. For example, Caveolin-3 is expressed specifically in ciliated cells, where it is necessary to properly localize proteins that regulate ciliary beat frequency (Krasteva et al., 2006). Moreover, the FoxJ1 transcription factor is expressed specifically in ciliated cells, where it governs the formation of cilia (You et al., 2004). In the absence of FoxJ1, ezrin-mediated anchoring of basal bodies fails, and cilia are not properly assembled (Gomperts et al., 2004; Huang et al., 2003).

Studies into molecular mechanisms of mucociliary epithelial development are hampered in mammals by the inaccessibility of the tissues, particularly during early stages. Curiously, a simple *in vivo* model system to facilitate such studies is provided by the aquatic embryos of amphibians. Similar to the airway, the entire epidermis of amphibian embryos develops as a salt-and-pepper mix of mucus-secreting goblet cells and ciliated cells (Fig. 1A-B; Fig. 2) (Billett and Gould, 1971; Nishikawa et al., 1992; Nokhbatolfoghahai et al., 2005; Steinman, 1968).

Several studies underscore the similarities between the amphibian embryonic epidermis and the vertebrate airway. First, goblet cells in both epithelia secrete mucus via an extensive exocytic apparatus, while ciliated cells bear numerous large cilia (Fig. 1A-B; Fig 2 (Billett and Gould, 1971; Steinman, 1968). Second, the many cilia atop ciliated cells beat coordinately and with a robust planar polarity, similar to that observed in the airway (Assheton, 1896; Konig and Hausen, 1993; Nokhbatolfoghahai et al., 2005; Twitty, 1928). This polarized ciliary beating can be readily observed by the movement of particles across the embryonic epidermis (See Supplemental Movies 1& 2). Third, ciliated cells are thought to transdifferentiate into goblet cells in the amphibian epidermis (Kessel et al., 1974; Nishikawa et al., 1992). Finally, there are important molecular similarities: Caveolin-3, FoxJ1 and Sox-family transcription factors are expressed specifically in ciliated cells of the *Xenopus* epidermis and likewise in ciliated cells of the airway (see Table 1; (Fawcett and Klymkowsky, 2004; Krasteva et al., 2006; Pohl and Knochel, 2004; Razani et al., 2002; You et al., 2004).

In contrast to the ciliated cells, very little study has been made of the non-ciliated cells of the *Xenopus* epidermis. Nonetheless, it is known that they fall into at least two categories, the large secretory cells and the smaller, scattered cells (Fig. 1B–C; (Billett and Gould, 1971; Nickells et al., 1988). The large secretory cells in the *Xenopus* epidermis are the predominant cell type, and they are known to secrete lectin-rich mucus (Billett and Gould, 1971; Nagata, 2005). The smaller, scattered cells are of unknown function, but have been shown to contain electron-dense granules (Billett and Gould, 1971). It remains unclear whether these small, scattered cells represent a single cell type or multiple cell types (Itoh et al., 1988; Montorzi et al., 2000; Nickells et al., 1988; Stubbs et al., 2006).

We report here the results of an *in situ* hybridization-based screen for differentially-expressed genes in the mucociliary epithelium of the *Xenopus* epidermis. We have identified over 100 genes expressed specifically in the various cell types. Many of these genes encode regulatory proteins likely to be involved in cell fate specification. Studies in the *Xenopus* epidermis show that specification of ciliated and small, scattered cells within this tissue are regulated by Notch signaling (Deblandre et al., 1999; Stubbs et al., 2006), so it is notable that several effectors of Notch signaling were found to be expressed specifically in one cell type or another. In addition, our screen identified very early markers for each of the cell types, and we show that Notch

signaling acts upstream of these early markers. Notch signaling also governs ciliated cell differentiation in the kidney (Liu et al., 2007; Ma and Jiang, 2007), so these results may be broadly relevant to ciliated epithelia. We also identified several structural proteins likely to be involved in terminal differentiation, and many of these proteins are also expressed by mucus-secreting goblet cells of the airway.

We have identified several new candidate ciliogenesis factors. GFP-fusion proteins revealed that TTC25 and Mig12 localize to the base of cilia and to ciliary axonemes. Mig12-GFP is especially notable because we find that it allows for simple visualization of the asymmetric morphology of basal bodies and thus revealing the planar polarization of basal bodies that underlies polarized ciliary beating (Frisch and Farbman, 1968; Mitchell et al., 2007). We show hear that with Mig12-GFP, such polarity can be assessed by confocal microscopy. Finally, we present experimental data to demonstrate that factors identified in ciliated cells in this screen are also required in the midline for normal neural tube closure. These results provide a foundation for future studies into the specification and differentiation of cell types in mucociliary epithelia.

Materials and Methods

High-throughput *in situ* hybridization

Whole-mount *in situ* hybridization was performed with digoxigenin (DIG)-labeled probes, as described by Harland (Sive et al., 2000). For the large scale in situ hybridization analysis, 6 staged embryos per probe were fixed and processed by hybridization reaction. Riboprobes were synthesized in 96-well plastic plates simultaneously with T7 or SP6 RNA polymerases, and subjected to hybridization. Hybridization and washing were processed by two automated machines (In situ Pro, Abimed) in parallel. Chromogenic reactions were manually performed with an alkaline phosphatase-coupled anti-DIG antibody and visualized by using BM purple (Roche Molecular Biochemicals).

Immunohistochemistry, phalloidin staining, and low-throughput *in situ* hybridization

For immunostaining, embryos were fixed in MEMFA, washed in TBST for 30 minutes at room temperature, then blocked in 10% FBS and 90% TBST (0.1% Triton X-100 in TBS). Primary antibodies were diluted in 10% FBS and 90% TBST. Antibodies used were monoclonal anti-Xeel (1:1000 dilution, Nagata, S., 2005) and monoclonal anti-alpha-tubulin (1:300, Sigma #T9062). Primary antibodies were detected with Alexa Fluor-488 goat anti-mouse immunoglobulin G (IgG), or Alexa Fluor-555 goat anti-mouse IgG (Molecular Probes) diluted 1:300 in FBS/TBST solution.

F-actin was analyzed using alexa-fluor 488 phalloidin (1:300 diluted in TBST, Invitrogen, #A12379). Phalloidin was added during secondary antibody incubation and washed off with TBST for 30 minutes at room temperature.

Specific *in situ* hybridizations were performed according to (Sive et al., 2000) with digoxygenin-labeled, antisense probes. Day one of the standard in situ protocol was altered as follows: embryos were washed out of MeOH into PBST, prehybridized for 1 hour at 60 C, then hybridized in antisense probe overnight at 60 C.

Morpholino and mRNA injection

Capped mRNA was synthesized using mMessage mMachine kits (Ambion). mRNA or antisense morpholino oligonucleotide (MO) was injected into one or two ventral blastomeres at the four-cell stage to target epidermis, or 2 dorsal cells at 4 cell stage to target neural tissue; MO's were injected at 10–40ng and phenotypes confirmed by injection of equivalent doses of

5 bp mismatch MO's. memGFP was injected at 300pg to confirm proper targeting of injection. Embryos were incubated until appropriate stages and then fixed in 1X MEMFA.

MO sequences used were as follows:

Mig12: TTTCCTTCAATAGTACAAATGGTCC;

Mig12 Mismatch: TTTCgTTgAATAcTACAAATGcTCC

TTC25: GGCGAGAGTTGGCGTTACCTTGAAG TTC

Mismatch: GGCcAGAcTTGcCGTTAgCTTcAAG

Imaging and Image Anylsis

Immunohistochemistry and phalloidin stained embryos were imaged in TBST on an inverted Zeiss LSM5 Pascal confocal microscope. Z-stacks were taken from the top of the cilia to the apical surface of the cell and cilia height were analyzed using LSM5 Pascal software. The images for bright field and fluorescence view (*in situs* + α-tubulin) were captured on a stereomicroscope (Leica MZ16FA). Images used throughout this study have been enhanced using Adobe Photoshop.

Electron microscopy was performed roughly according to (Billett and Gould, 1971) and (Steinman, 1968). Specimens for electron microscopy were fixed in a phosphate buffered 3% gluteraldehyde and then post-fixed in a phosphate buffered 2% osmium tetroxide. Tissue was then dehydrated in a stepwise manner. For transmission electron microscopy, the embryos were embedded in Araldite 502 resin and 50 nm sections were cut using an ultramicrotome. Scanning electron microscopy specimens were critical point dried and then mounted on stubs using silver paste. Afterwards they were sputter coated with 20 nm of platinum.

RESULTS AND DISCUSSION

Identification of differentially-expressed genes in a mucociliary epithelium

To identify new genes involved in the development of mucociliary epithelia, we performed *in situ* hybridization to over 950 randomly-chosen *Xenopus* cDNAs, searching for genes expressed differentially in the epidermis (Fig. 1E–G). Many genes produced a distinct pattern of dark spots on the light background of the embryo surface. Of these, some genes were expressed in a regularly spaced pattern (Fig. 1E; 3A–B), indicating specific expression in the regularly-spaced ciliated cells (Deblandre et al., 1999). Other genes were expressed in irregularly scattered cells (Fig. 1G; 3C), a pattern similar to the distribution of the small, scattered cells (Stubbs et al., 2006). Finally, many other genes produced a broad, dark stain with light spots, indicating expression in the large secretory cells, which we will refer to as goblet cells (Fig. 1F; 3D). Using this method, we identified over 100 differentially-expressed genes (Tables 2–4). An annotated, interactive list of all genes identified in this study is provided in Supplemental Table 1.

Genes expressed in goblet cells

To ask if our method reliably identified differentially-expressed genes, we first examined our dataset for "positive-control" genes that would be expected to be expressed in one cell type or the other. Our goblet cell dataset contained many genes that would be expected to be upregulated in secretory cells, including the membrane-trafficking proteins such as AP2 and Delta-COP, as well as several members of the Rab family of GTPases (Fig. 1F; Table 2). These included Rab6A, which has been implicated recently in controlling exocytosis (Gregoriev et al., 2007).

In goblet cells, we also found several regulatory proteins likely to be involved in the early specification of this cell type, including members of the Distalless, Gata, and Hes transcription factor families, as well as a member of the MAP kinase family. Given that Notch signals are involved in specification of cell types in the ciliated epidermis (Deblandre et al., 1999), Hes1 was a particularly interesting finding. Hes1 is involved in Notch signaling, and moreover, this gene is expressed strongly in the airway epithelium (Chen et al., 1997; van Tuyl et al., 2005). In addition to regulatory genes, we also identified several genes that contribute to the functioning of differentiated goblet cells, including several of the protein constituents of the mucus secreted by this epithelium (Table 2).

Most notably, we identified genes that are known to be important in other mucociliary epithelia. These include not only general factors known to be upregulated in the airway (e.g. serine proteases and calpain-2), but also some important effectors of airway physiology. We identified cytokeratin-18 in goblet cells, and this gene is expressed in mucus-secreting cells in the airway and is also implicated in airway pathogenesis (Chow et al., 1997; Nahm et al., 2002). We also identified intelectin-2 as a gene expressed specifically in goblet cells of the *Xenopus* epidermis (Fig. 4). This gene, also called Xeel, was previously identified as being specifically expressed in the goblet cells (Nagata, 2005; Nagata et al., 2003), and it is especially intriguing for two reasons. First, intelectin-2 is expressed in the human airway and is overexpressed in mouse asthma models and is also overexpressed in human asthma patients (Kuperman et al., 2005). Intelectin-2 is also a key component of the gut mucociliary system, where it is involved in resistance to parasite infection (Pemberton et al., 2004).

We observed that the secretory vesicles of the *Xenopus* epidermal goblet cells can be readily visualized by expression of membrane-tethered GFP (memGFP; Fig. 4A–B). Using this method, we observed that most of the vesicles on the *Xenopus* epidermal goblet cells are filled with intelectin-2 protein (Fig. 4A–B), but we also observed many vesicles that did not contain intelectin-2 (Fig. 4A, arrowhead). These vesicles may simply have already discharged their contents, or alternatively, this finding could indicate the presence of a population of secretory vesicles that lack intelectin-2. TEM and SEM revealed the presence of many empty vesicles at the apical surface of goblet cells, suggesting the former interpretation is the correct one (Fig. 4C, arrowhead; 2B, arrowhead).

This TEM analysis also revealed vesicles in various stages of exocytosis (Fig. 4C–E), including what appear to be intermediate steps in the membrane fusion process for vesicle release (Fig. 4D). Such outpocketing of thin membrane has been observed in other cell types undergoing exocytosis of very large vesicles, for example mast cells (Lawson et al., 1977).

Finally, we examined the distribution of F-actin in goblet cells using fluorescent phalloidin. The phalloidin staining did not highlight the secretory vesicles in this cell type (Fig. 1C). Rather, the phalloidin strongly labeled the many small ridges that have been observed by SEM to cover the apical surface of these cells (2A-B (Nishikawa et al., 1992). These preliminary observations and the many genes identified in this cell type lay a foundation for future studies of the mechanisms of mucus secretion from goblet cells.

Genes expressed in ciliated cells

We next examined our ciliated cell dataset for known ciliary proteins, and we found several, including Rootletin, Centrin, Tektin, and Shippo, among others (Fig. 1E; Table 3). These "positive-control" genes demonstrate the ability of our screen to accurately identify cell-type specific factors. Many of the genes that we identified as expressed in ciliated epidermal cells were also found to be expressed in the otic vesicle and the ventral midline of the neural plate (Fig. 5A–B).

We identified several regulatory proteins in ciliated cells that may be involved in their specification, including transcription factors and Ras-family GTPases. Given the role of Sox genes in ciliated cell development, it was interesting to find Med12, which is a member of the Mediator complex and is a known co-factor for Sox transcription factors (Fawcett and Klymkowsky, 2004; Rau et al., 2006). It was also exciting to find an interleukin receptor gene expressed specifically in ciliated cells of the *Xenopus* epidermis (Table 3), because interleukins control homeostasis and transdifferentiation in the airway epithelium (Laoukili et al., 2001; Vermeer et al., 2003).

In ciliated cells, we also identified several proteins with functions related to the microtubule cytoskeleton. Of particular interest among these is a β-6-tubulin gene. There are a great many tubulin genes (Luduena, 1998), and at present the only one known to be expressed specifically in ciliated cells of this mucociliary epithelium is an α-tubulin (Deblandre et al., 1999). The tubulin gene identified here is of interest because a subset of the β-tubulin genes that contribute importantly to ciliary motility contain a unique c-terminal motif (Nielsen et al., 2001; Vent et al., 2005). This c-terminal motif is present in the β-3-tubulin gene we identified (not shown). Coordinated beating is an important aspect of mucociliary epithelia (See Supplemental Movies 1& 2), and this finding will facilitate future studies of ciliary motility in this tissue.

Finally, we examined our differentially-expressed genes at a variety of time-points, allowing us to place them in a temporal hierarchy. Among the earliest-expressed genes in ciliated cells is a transcript with weak homology to a testis-expressed gene in the mouse, TEX15. We found that this gene was expressed specifically in ciliated cells long before these cells display overt signs of differentiation. For example, presumptive ciliated cells express acetylated α-tubulin beginning about 18 hours after fertilization (Chu and Klymkowsky, 1989), but these cells express the TEX15-related gene much earlier, around 12 hours post-fertilization. In addition, this gene is expressed strongly in other ciliated cells, such as the midline of the neural plate and the developing inner ear (Fig. 5A–B). Because expression of constitutively-active Notch[icd] in the epidermis eliminates ciliated cells (Deblandre et al., 1999), we used our TEX15-related gene to ask how Notch might exert its effect early in development. We found that Notch[icd] potently eliminated the early expression of TEX15, indicating that Notch signaling acts at the earliest stages of ciliated cell specification (Fig. 5C–D).

Genes expressed in the scattered, small cells

We also identified several genes expressed exclusively in the scattered population of specialized cells in the epidermis (Table 4). It is not clear that this population of cells in the amphibian epidermis has a proper counterpart in other mucociliary epithelia, though it is conceivable that they are related to specialized secretory cell types. Indeed, by ultrastructure, these scattered cells in the *Xenopus* epidermis resemble Clara cells of the lung, in that both contain numerous electron-dense granules apically (Billett and Gould, 1971;Stinson and Loosli, 1978).

We examined the apical surface of these cells by confocal microscopy. The vesicles on scattered secretory cells differ from those of the goblet cells; vesicles on the former are larger in diameter and, curiously, are not readily observable by expression of membrane-GFP (not shown). On the other hand, these vesicles are strongly labeled by phalloidin staining, again in contrast to the vesicles on goblet cells (Fig. 1c'). It is not clear if these scattered cells represent a single cell type, because by SEM, we and others have observed small cells that were neither ciliated nor apparently secretory (Fig. 2A and (Montorzi et al., 2000)). It is possible that these cells undergo periodic exocytic events, and so in fixed samples they will appear to be secretory at some times, but not at other times. Because activation of Notch signaling uniformly eliminates all irregularly-spaced, scattered cells in the epidermis (Stubbs et al., 2006), we will consider these to be a single population for the purposes of this study.

We identified several transcription factors that are differentially-expressed in this population, and these included Sox- and Fox-family transcription factors. We used antibody staining against α-tubulin to confirm that these genes were not expressed in ciliated cells (Fig. 6A). Given that this population of cells, like the ciliated cells, is negatively regulated by Notch signals (Stubbs et al., 2006), we asked if the expression of transcription factors identified here may function downstream of Notch signals. Indeed, we found that expression of Foxa 1, CP2, and other transcription factors were eliminated by expression of constitutively-active Notch (Fig. 6B–E and data not shown). Finally, our screen also identified very early markers of differentiation in this population of cells. We found that the solute carrier Slc16a3, like TEX15 in the ciliated cells, is expressed in scattered secretory cells as early as 12 hours post-fertilization. This early expression of Slc16a3 was reduced by expression of Notch[icd] (Fig. 6F–G).

Validation of putative ciliogenesis factors

Recent reports have demonstrated a central role for cilia in a wide variety of developmental processes. In addition to their established mechanical roles in mucociliary epithelia, it is now clear that these organelles are required for the transduction of molecular signals that govern the patterning and morphogenesis of vertebrate embryos (Huangfu et al., 2003; Park et al., 2006c; Scholey and Anderson, 2006). Given the ease and rapidity with which the *Xenopus* embryo can be manipulated, the ciliated epidermis provides an excellent *in vivo* model system for studies of ciliogenesis. Indeed, our screen identified several genes that are likely to be important for ciliogenesis. Recent bioinformatics studies have defined the putative protein complement of cilia, called the "ciliome"(Gherman et al., 2006; Inglis et al., 2006). Our screen identified several genes encoding proteins of unknown function that are present in the ciliome, including CCDC11 and TTC25 (Table 3). The presence of a protein in the ciliome does not alone demonstrate a requirement for that protein in ciliogenesis, so we exploited the simplicity of gene knockdowns in the *Xenopus* epidermis to perform functional studies of putative ciliogenesis factors.

We focused on TTC25, which contains several tetratricopeptide repeats, and such repeats are also found in the intraflagellar transport (IFT) protein, Polaris and in the ciliopathic Bardet-Beidel syndrome gene BBS8 (Ansley et al., 2003; Haycraft et al., 2001). We first combined *in situ* hybridization with anti-tubulin immunostaining to confirm that the cells expressing TTC25 were in fact ciliated cells (Fig. 8A–B). In vertebrates, Polaris is present at basal bodies and also in the ciliary axoneme, while BBS8 is present only at basal bodies (Ansley et al., 2003; Taulman et al., 2001). We therefore generated a TTC25-GFP fusion protein and expressed it by mRNA injection in order to observe its subcellular localization. We observed that TTC25-GFP localized to both ciliary axonemes and to foci in the apical cell surface, presumably basal bodies (Fig. 7B), similar to the pattern observed for Polaris. As a reference, we observed that the PCP effector protein Inturned localizes to the apical surface of ciliated cells, but is not present in ciliary axonemes (Fig. 7A;(Park et al., 2006c).

Finally, in order to assess the requirement for TTC25 in ciliogenesis, we generated antisense morpholino-oligonucleotides (MOs) to disrupt the proper splicing of this gene. Injection of the MO resulted in defective cilia assembly as assessed by confocal microscopy of α-tubulin (Fig. 8C–D). SEM analysis revealed that TTC25 morphant cells formed far fewer cilia and what cilia were present were extremely short (Fig. 10A, B). In most morphant cells, a number of very short cilia-like projections could often be observed (Fig. 10B). In contrast, injection of equal amounts of a MO that was a 5-base-pair mismatch of the TTC25 MO sequence had no effect on ciliogenesis, even when observed ultrastructurally (Fig. 10D, E).

Identification and validation of ciliogenesis factors not present in the current ciliome

The establishment of the ciliome has been an important step in our understanding of ciliary assembly and function (Gherman et al., 2006; Inglis et al., 2006). However, it is clear that many proteins that have not been identified in the ciliome will be crucial for normal ciliogenesis. For example, normal cilia formation requires assembly of a specialized apical actin cytoskeleton (Boisvieux-Ulrich et al., 1990), and we have shown that the planar cell polarity effectors Inturned and Fuzzy govern ciliogenesis by controlling assembly of this actin network (Park et al., 2006c). However, neither of those proteins is present in the ciliome. It was therefore intriguing to us that we identified potential regulators of the microtubule cytoskeleton in ciliated cells that are *not* present in the current ciliome, including doublecortin domain-containing 2 (Coquelle et al., 2006) and the MID1-interacting protein, Mig12 (Berti et al., 2004).

We confirmed that Mig12 was expressed in ciliated cells of the epidermis (Fig. 9A), though with extended staining, weak expression could be detected in goblet cells. To ask if Mig12 may be involved in ciliogenesis, we generated a Mig12-GFP fusion protein. Mig12-GFP localized strongly to the base of cilia (Fig. 7C). Indeed, this localization of Mig12-GFP was so specific that the planar polarization of the ciliary basal apparatus was readily apparent by confocal imaging (Fig. 7c6). This alignment of basal bodies previously has been observed in TEM sections, and it underlies directed ciliary beating (Mitchell et al., 2007). As such, Mig12-GFP will be a useful reagent for future studies of planar polarization in ciliated cells. Under normal imaging conditions, Mig12-GFP specifically labels the base of cilia, however when detection levels are increased, Mig12-GFP can be detected in ciliary axonemes (Fig. 7c4–c5). By comparison, Inturned-GFP is not found in ciliary axonemes under any conditions (Fig. 7A).

We then designed an antisense MO to suppress translation of endogenous Mig12. Using targeted injection, we generated mosaic animals in which membrane-GFP labeled epidermal cells contained the MO, while unlabeled neighboring cells did not. We observed a near-total suppression of ciliogenesis in cells containing the MO, while uninjected cells nearby developed normal cilia (Fig. 9B–D). Again SEM analysis confirmed that ciliogenesis was severely compromised in Mig12 morphant cells, but was unaffected in cells injected with a 5base-pair mismatch of the Mig12 MO (Fig. 10A, C, D, F). Together, these results demonstrate a requirement for Mig12 in ciliogenesis, and highlight the important contributions made by proteins not present in the current ciliome.

Novel ciliogenesis factors are required for neural tube closure

Finally, we asked if factors identified in the developing ciliated epidermis were more generally required for ciliogenesis. To test this possibility, we exploited the fact that normal ciliogenesis in the developing central nervous system is required for neural tube closure (Huangfu et al., 2003; Park et al., 2006c; Wallingford, 2006; Zohn et al., 2005). During our *in situ* screening, we observed that both TTC25 and Mig12 were expressed in the ventral midline of the developing neural plate (Fig. 11A and D, arrows) Mig12 has also been shown to be expressed strongly in this region in the mouse embryo (Berti et al., 2004). We therefore used targeted injection of MOs to disrupt either TTC25 or Mig12 specifically to the neural plate. Such targeted injection of either TTC25 or Mig12 MOs potently disrupted neural tube closure (Fig. 10B–C and 10E–F). Injection of 5-bp mismatch MOs against either gene had no effect on development (not shown). The neurulation phenotype of Mig12 and TTC25 morphants is indistinguishable from that of MOs against known ciliogenesis factors such as Inturned or Fuzzy (Park et al., 2006c), and these neural tube defects are strikingly similar to those of mouse mutants with defective ciliogenesis (Huangfu et al., 2003; Zohn et al., 2005). These data thus suggest that factors identified by our screen play broad roles in ciliogenesis.

CONCLUSION

We have defined here a suite of genes expressed differentially in mucus-secreting goblet cells or in ciliated cells of a simple mucociliary epithelium. Large-scale *in situ* hybridization-based screens have been performed previously in *Xenopus* embryos, and some genes with specific patterns in the epidermis were identified (Pollet et al., 2003; Pollet et al., 2005). However, our screen focused specifically on differential expression in the ciliated epidermis, and the suites of genes identified here do not overlap with those previously identified (e.g. compare Tables 1 and 3). Additional *in situ* hybridization-based screening will be useful for identifying additional players in mucociliary epithelial development.

The genes identified here encode regulatory proteins likely to impact early specification and also structural elements likely to be involved in later differentiation. These data provide molecular evidence of the strong similarity between the *Xenopus* ciliated epidermis and other vertebrate mucociliary epithelia. Most notably, this study has identified novel ciliogenesis factors that are not present in the current ciliome. Several of the genes we identified in our screen have also been found recently to be upregulated during airway differentiation (see (Ross et al., 2007)), while other identified genes are associated with airway disorders (Kuperman et al., 2005). The screen and our functional studies thus provide a foundation for further work and establish the *Xenopus* tadpole epidermis as a facile model system for rapid, *in vivo* studies of mucociliary epithelia.

Supplementary Material

Refer to Web version on PubMed Central for supplementary material.

References

Altmann CR, Bell E, Sczyrba A, Pun J, Bekiranov S, Gaasterland T, Brivanlou AH. Microarray-based analysis of early development in Xenopus laevis. Dev Biol 2001;236:64–75. [PubMed: 11456444]

Ansley SJ, Badano JL, Blacque OE, Hill J, Hoskins BE, Leitch CC, Kim JC, Ross AJ, Eichers ER, Teslovich TM, Mah AK, Johnsen RC, Cavender JC, Lewis RA, Leroux MR, Beales PL, Katsanis N. Basal body dysfunction is a likely cause of pleiotropic Bardet-Biedl syndrome. Nature 2003;425:628–33. [PubMed: 14520415]

Assheton R. Notes on the ciliation of the ectoderm of the amphibian embryo. Q J Microsc Sci 1896;38:465–484.

Berti C, Fontanella B, Ferrentino R, Meroni G. Mig12, a novel Opitz syndrome gene product partner, is expressed in the embryonic ventral midline and co-operates with Mid1 to bundle and stabilize microtubules. BMC Cell Biol 2004;5:9. [PubMed: 15070402]

Billett FS, Gould RP. Fine structural changes in the differentiating epidermis of Xenopus laevis embryos. J Anat 1971;108:465–80. [PubMed: 5575314]

Boisvieux-Ulrich E, Laine MC, Sandoz D. Cytochalasin D inhibits basal body migration and ciliary elongation in quail oviduct epithelium. Cell Tissue Res 1990;259:443–54. [PubMed: 2317839]

Chen H, Thiagalingam A, Chopra H, Borges MW, Feder JN, Nelkin BD, Baylin SB, Ball DW. Conservation of the Drosophila lateral inhibition pathway in human lung cancer: a hairy-related protein (HES-1) directly represses achaete-scute homolog-1 expression. Proc Natl Acad Sci U S A 1997;94:5355–60. [PubMed: 9144241]

Chow YH, O'Brodovich H, Plumb J, Wen Y, Sohn KJ, Lu Z, Zhang F, Lukacs GL, Tanswell AK, Hui CC, Buchwald M, Hu J. Development of an epithelium-specific expression cassette with human DNA regulatory elements for transgene expression in lung airways. Proc Natl Acad Sci U S A 1997;94:14695–700. [PubMed: 9405675]

Chu DT, Klymkowsky MW. The appearance of acetylated alpha-tubulin during early development and cellular differentiation in Xenopus. Dev Biol 1989;136:104–17. [PubMed: 2680681]

Coquelle FM, Levy T, Bergmann S, Wolf SG, Bar-El D, Sapir T, Brody Y, Orr I, Barkai N, Eichele G, Reiner O. Common and divergent roles for members of the mouse DCX superfamily. Cell Cycle 2006;5:976–83. [PubMed: 16628014]

Deblandre GA, Wettstein DA, Koyano-Nakagawa N, Kintner C. A two-step mechanism generates the spacing pattern of the ciliated cells in the skin of Xenopus embryos. Development 1999;126:4715–28. [PubMed: 10518489]

Fawcett SR, Klymkowsky MW. Embryonic expression of Xenopus laevis SOX7. Gene Expr Patterns 2004;4:29–33. [PubMed: 14678825]

Frisch D, Farbman AI. Developmennt of order during ciliogenesis. Ant Rec 1968;162:221–232.

Gherman A, Davis EE, Katsanis N. The ciliary proteome database: an integrated community resource for the genetic and functional dissection of cilia. Nat Genet 2006;38:961–2. [PubMed: 16940995]

Gomperts BN, Gong-Cooper X, Hackett BP. Foxj1 regulates basal body anchoring to the cytoskeleton of ciliated pulmonary epithelial cells. J Cell Sci 2004;117:1329–37. [PubMed: 14996907]

Grigoriev I, Splinter D, Keijzer N, Wulf PS, Demmers J, Ohtsuka T, Modesti M, Maly IV, Grosveld F, Hoogenraad CC, Akhmanova A. Rab6 regulates transport and targeting of exocytotic carriers. Dev Cell 2007;13:305–14. [PubMed: 17681140]

Haycraft CJ, Swoboda P, Taulman PD, Thomas JH, Yoder BK. The C. elegans homolog of the murine cystic kidney disease gene Tg737 functions in a ciliogenic pathway and is disrupted in osm-5 mutant worms. Development 2001;128:1493–505. [PubMed: 11290289]

Huang T, You Y, Spoor MS, Richer EJ, Kudva VV, Paige RC, Seiler MP, Liebler JM, Zabner J, Plopper CG, Brody SL. Foxj1 is required for apical localization of ezrin in airway epithelial cells. J Cell Sci 2003;116:4935–45. [PubMed: 14625387]

Huangfu D, Anderson KV. Cilia and Hedgehog responsiveness in the mouse. Proc Natl Acad Sci U S A 2005;102:11325–30. [PubMed: 16061793]

Huangfu D, Liu A, Rakeman AS, Murcia NS, Niswander L, Anderson KV. Hedgehog signalling in the mouse requires intraflagellar transport proteins. Nature 2003;426:83–7. [PubMed: 14603322]

Huynh MH, Hong H, Delovitch S, Desser S, Ringuette M. Association of SPARC (osteonectin, BM-40) with extracellular and intracellular components of the ciliated surface ectoderm of Xenopus embryos. Cell Motil Cytoskeleton 2000;47:154–62. [PubMed: 11013395]

Inglis PN, Boroevich KA, Leroux MR. Piecing together a ciliome. Trends Genet 2006;22:491–500. [PubMed: 16860433]

Itoh K, Yamashita A, Kubota HY. The expression of epidermal antigens in Xenopus laevis. Development 1988;104:1–14. [PubMed: 3075541]

Kessel RG, Beams HW, Shih CY. The origin, distribution and disappearance of surface cilia during embryonic development of Rana pipiens as revealed by scanning electron microscopy. Am J Anat 1974;141:341–59. [PubMed: 4548631]

Knowles MR, Boucher RC. Mucus clearance as a primary innate defense mechanism for mammalian airways. J Clin Invest 2002;109:571–7. [PubMed: 11877463]

Konig G, Hausen P. Planar polarity in the ciliated epidermis of Xenopus embryos. Dev Biol 1993;160:355–68. [PubMed: 8253269]

Krasteva G, Pfeil U, Filip AM, Lips KS, Kummer W, Konig P. Caveolin-3 and eNOS colocalize and interact in ciliated airway epithelial cells in the rat. Int J Biochem Cell Biol. 2006

Kuperman DA, Lewis CC, Woodruff PG, Rodriguez MW, Yang YH, Dolganov GM, Fahy JV, Erle DJ. Dissecting asthma using focused transgenic modeling and functional genomics. J Allergy Clin Immunol 2005;116:305–11. [PubMed: 16083784]

Laoukili J, Perret E, Willems T, Minty A, Parthoens E, Houcine O, Coste A, Jorissen M, Marano F, Caput D, Tournier F. IL-13 alters mucociliary differentiation and ciliary beating of human respiratory epithelial cells. J Clin Invest 2001;108:1817–24. [PubMed: 11748265]

Lawson D, Raff MC, Gomperts B, Fewtrell C, Gilula NB. Molecular events during membrane fusion. A study of exocytosis in rat peritoneal mast cells. J Cell Biol 1977;72:242–59. [PubMed: 319098]

Liu Y, Pathak N, Kramer-Zucker A, Drummond IA. Notch signaling controls the differentiation of transporting epithelia and multiciliated cells in the zebrafish pronephros. Development 2007;134:1111–22. [PubMed: 17287248]

Luduena RF. Multiple forms of tubulin: different gene products and covalent modifications. Int Rev Cytol 1998;178:207–75. [PubMed: 9348671]

Ma M, Jiang YJ. Jagged2a-notch signaling mediates cell fate choice in the zebrafish pronephric duct. PLoS Genet 2007;3:e18. [PubMed: 17257056]

Mitchell B, Jacobs R, Li J, Chien S, Kintner C. A positive feedback mechanism governs the polarity and motion of motile cilia. Nature 2007;447:97–101. [PubMed: 17450123]

Montorzi M, Burgos MH, Falchuk KH. Xenopus laevis embryo development: arrest of epidermal cell differentiation by the chelating agent 1,10-phenanthroline. Mol Reprod Dev 2000;55:75–2. [PubMed: 10602276]

Nagata S. Isolation, characterization, and extra-embryonic secretion of the Xenopus laevis embryonic epidermal lectin, XEEL. Glycobiology 2005;15:281–90. [PubMed: 15537792]

Nagata S, Nakanishi M, Nanba R, Fujita N. Developmental expression of XEEL, a novel molecule of the Xenopus oocyte cortical granule lectin family. Dev Genes Evol 2003;213:368–70. [PubMed: 12802587]

Nahm DH, Lee YE, Yim EJ, Park HS, Yim H, Kang Y, Kim JK. Identification of cytokeratin 18 as a bronchial epithelial autoantigen associated with nonallergic asthma. Am J Respir Crit Care Med 2002;165:1536–9. [PubMed: 12045129]

Nickells RW, Cavey MJ, Browder LW. The effects of heat shock on the morphology and protein synthesis of the epidermis of Xenopus laevis larvae. J Cell Biol 1988;106:905–14. [PubMed: 3346329]

Nielsen MG, Turner FR, Hutchens JA, Raff EC. Axoneme-specific beta-tubulin specialization: a conserved C-terminal motif specifies the central pair. Curr Biol 2001;11:529–33. [PubMed: 11413005]

Nishikawa S, Hirata J, Sasaki F. Fate of ciliated epidermal cells during early development of Xenopus laevis using whole-mount immunostaining with an antibody against chondroitin 6-sulfate proteoglycan and anti-tubulin: transdifferentiation or metaplasia of amphibian epidermis. Histochemistry 1992;98:355–8. [PubMed: 1293075]

Nokhbatolfoghahai M, Downie JR, Clelland AK, Rennison K. The surface ciliation of anuran amphibian embryos and early larvae: Patterns, timing differences and functions. Journal of Natural History 2005;39:887–929.

Park KS, Wells JM, Zorn AM, Wert SE, Laubach VE, Fernandez LG, Whitsett JA. Transdifferentiation of ciliated cells during repair of the respiratory epithelium. Am J Respir Cell Mol Biol 2006a;34:151–7. [PubMed: 16239640]

Park KS, Wells JM, Zorn AM, Wert SE, Whitsett JA. Sox17 influences the differentiation of respiratory epithelial cells. Dev Biol 2006b;294:192–202. [PubMed: 16574095]

Park TJ, Haigo SL, Wallingford JB. Ciliogenesis defects in embryos lacking inturned or fuzzy function are associated with failure of planar cell polarity and Hedgehog signaling. Nat Genet 2006c;38:303–11. [PubMed: 16493421]

Pemberton AD, Knight PA, Gamble J, Colledge WH, Lee JK, Pierce M, Miller HR. Innate BALB/c enteric epithelial responses to Trichinella spiralis: inducible expression of a novel goblet cell lectin, intelectin-2, and its natural deletion in C57BL/10 mice. J Immunol 2004;173:1894–901. [PubMed: 15265922]

Pohl BS, Knochel W. Isolation and developmental expression of Xenopus FoxJ1 and FoxK1. Dev Genes Evol 2004;214:200–5. [PubMed: 14986136]

Pollet N, Delius H, Niehrs C. In situ analysis of gene expression in Xenopus embryos. C R Biol 2003;326:1011–7. [PubMed: 14744108]

Pollet N, Muncke N, Verbeek B, Li Y, Fenger U, Delius H, Niehrs C. An atlas of differential gene expression during early Xenopus embryogenesis. Mech Dev 2005;122:365–439. [PubMed: 15763213]

Raji AR, Naserpour M. Light and Electron Microscopic Studies of the Trachea in the One-Humped Camel (Camelus dromedarius). Anat Histol Embryol 2007;36:10–3. [PubMed: 17266660]

Rau MJ, Fischer S, Neumann CJ. Zebrafish Trap230/Med12 is required as a coactivator for Sox9-dependent neural crest, cartilage and ear development. Dev Biol 2006;296:83–93. [PubMed: 16712834]

Razani B, Park DS, Miyanaga Y, Ghatpande A, Cohen J, Wang XB, Scherer PE, Evans T, Lisanti MP. Molecular cloning and developmental expression of the caveolin gene family in the amphibian Xenopus laevis. Biochemistry 2002;41:7914–24. [PubMed: 12069580]

Rogers DF. The airway goblet cell. Int J Biochem Cell Biol 2003;35:1–6. [PubMed: 12467641]

Ross AJ, Dailey LA, Brighton LE, Devlin RB. Transcriptional Profiling of Mucociliary Differentiation in Human Airway Epithelial Cells. Am J Respir Cell Mol Biol. 2007

Scholey JM, Anderson KV. Intraflagellar transport and cilium-based signaling. Cell 2006;125:439–42. [PubMed: 16678091]

Shin JB, Adams D, Paukert M, Siba M, Sidi S, Levin M, Gillespie PG, Grunder S. Xenopus TRPN1 (NOMPC) localizes to microtubule-based cilia in epithelial cells, including inner-ear hair cells. Proc Natl Acad Sci U S A 2005;102:12572–7. [PubMed: 16116094]

Sive, HL.; Grainger, RM.; Harland, RM. Early Development of *Xenopus laevis*: A Laboratory Manual. Cold Spring Harbor Press; Cold Spring Harbor, N.Y: 2000.

Steinman RM. An electron microscopic study of ciliogenesis in developing epidermis and trachea in the embryo of Xenopus laevis. Am J Anat 1968;122:19–55. [PubMed: 5654501]

Stinson SF, Loosli CG. Ultrastructural evidence concerning the mode of secretion of electron-dense granules by Clara cells. J Anat 1978;127:291–8. [PubMed: 721691]

Stubbs JL, Davidson L, Keller R, Kintner C. Radial intercalation of ciliated cells during Xenopus skin development. Development 2006;133:2507–15. [PubMed: 16728476]

Taulman PD, Haycraft CJ, Balkovetz DF, Yoder BK. Polaris, a protein involved in left-right axis patterning, localizes to basal bodies and cilia. Mol Biol Cell 2001;12:589–99. [PubMed: 11251073]

Toskala E, Smiley-Jewell SM, Wong VJ, King D, Plopper CG. Temporal and spatial distribution of ciliogenesis in the tracheobronchial airways of mice. Am J Physiol Lung Cell Mol Physiol 2005;289:L454–9. [PubMed: 15879461]

Twitty VC. Experimental studies on the ciliary action of amphibian embryos. J Exp Zool 1928;50:319–344.

van Tuyl M, Groenman F, Kuliszewski M, Ridsdale R, Wang J, Tibboel D, Post M. Overexpression of lunatic fringe does not affect epithelial cell differentiation in the developing mouse lung. Am J Physiol Lung Cell Mol Physiol 2005;288:L672–82. [PubMed: 15591414]

Vent J, Wyatt TA, Smith DD, Banerjee A, Luduena RF, Sisson JH, Hallworth R. Direct involvement of the isotype-specific C-terminus of beta tubulin in ciliary beating. J Cell Sci 2005;118:4333–41. [PubMed: 16159957]

Vermeer PD, Harson R, Einwalter LA, Moninger T, Zabner J. Interleukin-9 induces goblet cell hyperplasia during repair of human airway epithelia. Am J Respir Cell Mol Biol 2003;28:286–95. [PubMed: 12594054]

Wallingford JB. Planar cell polarity, ciliogenesis and neural tube defects. Hum Mol Genet 2006;15(Spec No 2):R227–34. [PubMed: 16987888]

Wanner A. The role of mucociliary dysfunction in bronchial asthma. Am J Med 1979;67:477–85. [PubMed: 382847]

Watkins DN, Berman DM, Burkholder SG, Wang B, Beachy PA, Baylin SB. Hedgehog signalling within airway epithelial progenitors and in small-cell lung cancer. Nature 2003;422:313–7. [PubMed: 12629553]

You Y, Huang T, Richer EJ, Schmidt JE, Zabner J, Borok Z, Brody SL. Role of f-box factor foxj1 in differentiation of ciliated airway epithelial cells. Am J Physiol Lung Cell Mol Physiol 2004;286:L650–7. [PubMed: 12818891]

Zohn IE, Anderson KV, Niswander L. Using genomewide mutagenesis screens to identify the genes required for neural tube closure in the mouse. Birth Defects Res A Clin Mol Teratol 2005;73:583–90. [PubMed: 15971254]
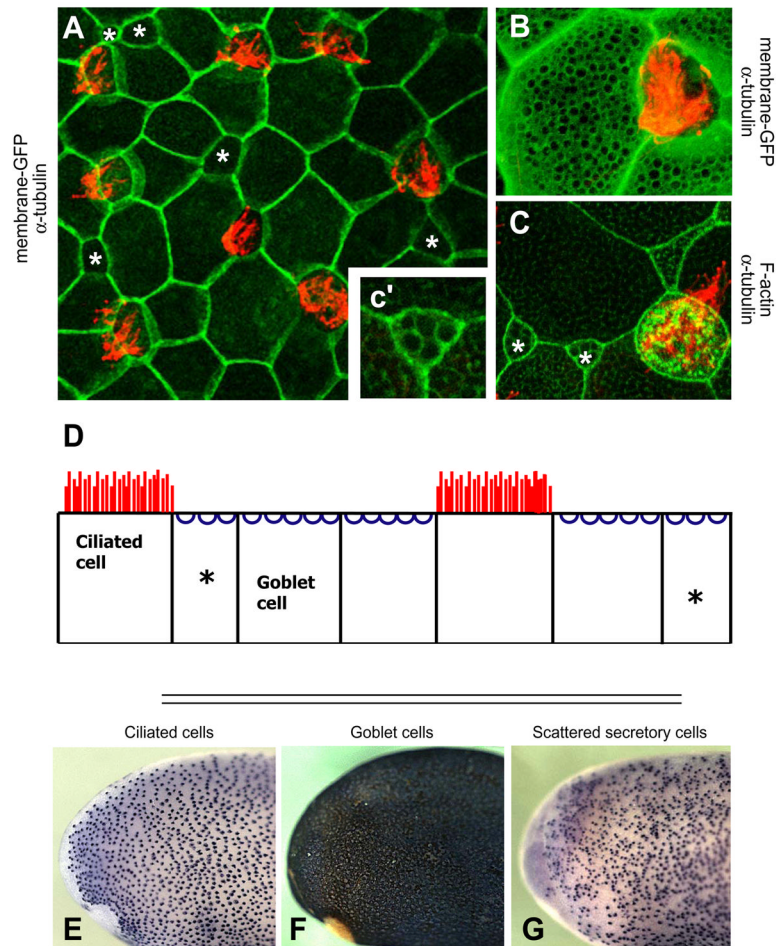
Figure 1. A screen for differentially-expressed genes in a mucociliary epithelium
A. The *Xenopus* epidermis is a salt-and-pepper mix of mucus-secreting goblet cells and ciliated cells. Ciliated cells are marked by red α-tubulin staining. Small secretory cells are labeled with an asterisk. All other cells are goblet cells. **B.** At higher magnification, membrane-GFP (green) reveals numerous exocytic vesicles at the apical surface of goblet cells, and α-tubulin staining (red) reveals cilia. **C.** The vesicles of small secretory cells are shown by phalloidin stain (green) and a neighboring ciliated cell is marked by alpha-tubulin stain (red). **c'.** A high magnification view of a small secretory cell shows visible vesicles. **D.** A diagram of cell types in the *Xenopus* epidermis. Goblet cells are the predominant cell type. Ciliated and small secretory cells (asterisks) are scattered throughout. **E.** *In situ* hybridization for genes expressed in ciliated cells produces regularly spaced dark spots on a light background. **F.** Genes expressed in goblet cells produce a reciprocal pattern. **G.** Small secretory cells are visible as unevenly scattered dark spots. The full set of differentially-expressed genes can be found in Supplemental Table 1.
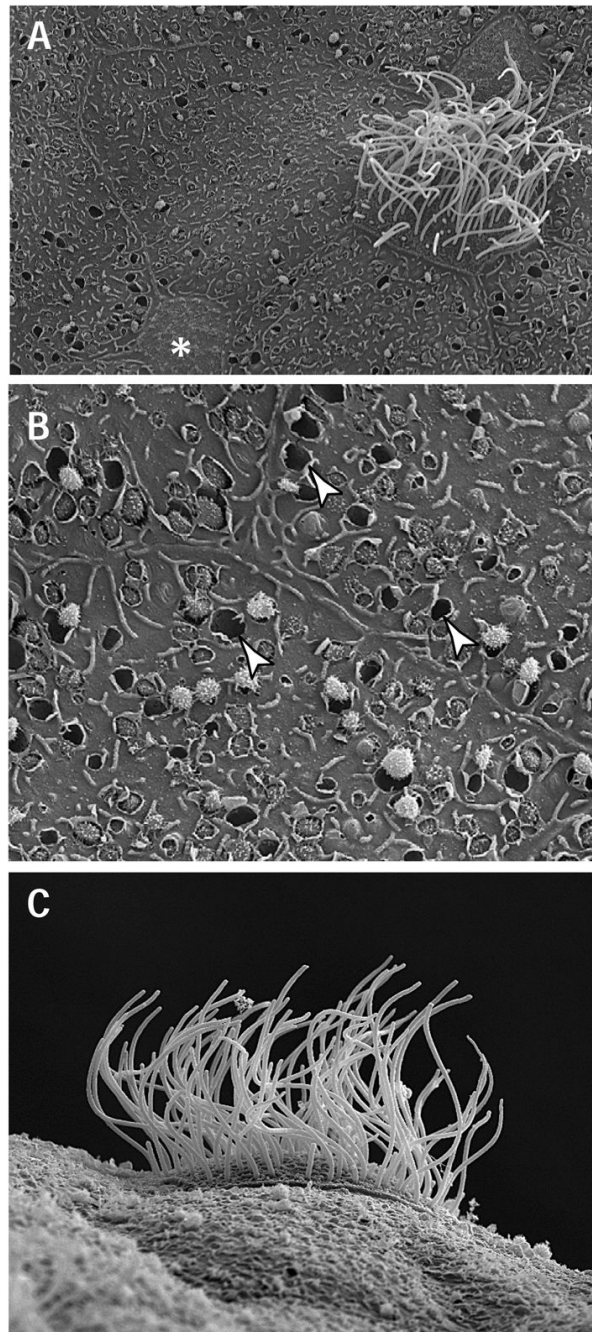
Figure 2. Ultrastructure of the Xenopus epidermis
A. View of mucociliary epithelium including a ciliated cell, small secretory cell (marked by *) and several large goblet cells. **B.** Goblet cells contain empty vesicles, noted with arrowheads, and vesicles with secretory granules being exocytosed. **C.** Lateral view of a ciliated cell, showing the many motile, apical cilia.
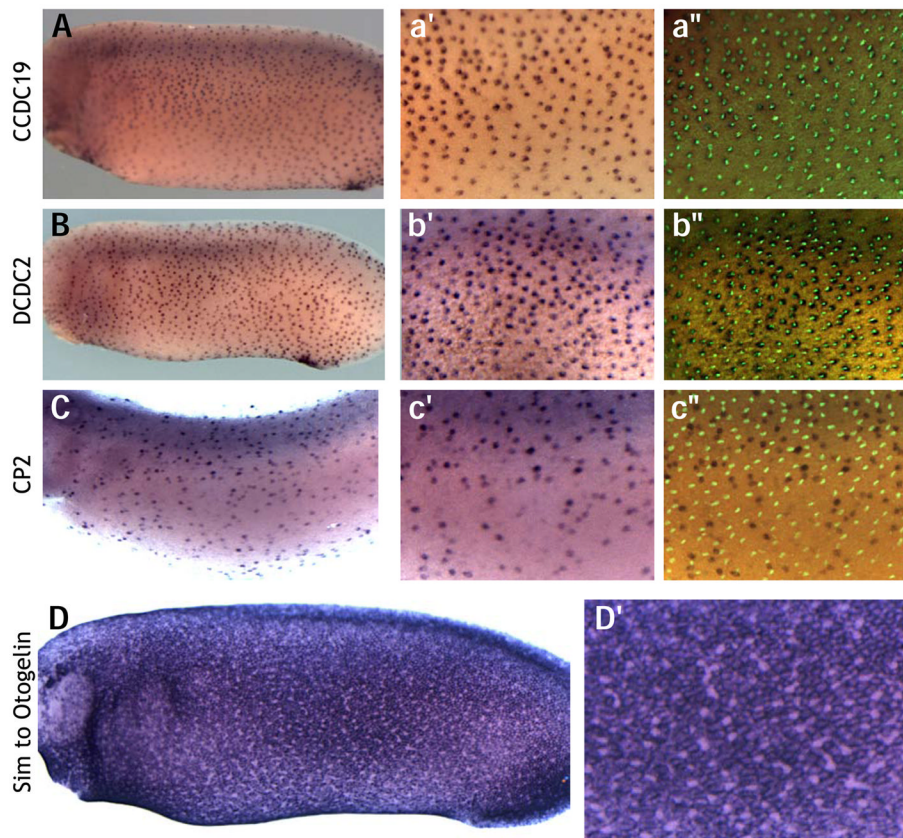
Figure 3. Representative Expression patterns from screen

Expression of Coiled-coil-domain containing 19, (**A**) and Doublecortin domain-containing-2 (**B**) in ciliated cells are evenly spaced and colocalize with α-tubulin marking cilia. **C.** The transcription factor CP2 is expressed in the scattered secretory cells, and its expression does not colocalize with cilia. **D.** Similar to Otogelin is expressed in mucus secreting goblet cells covering much of the epidermis. High magnification view reveals absence of expression in scattered secretory and ciliated cells.
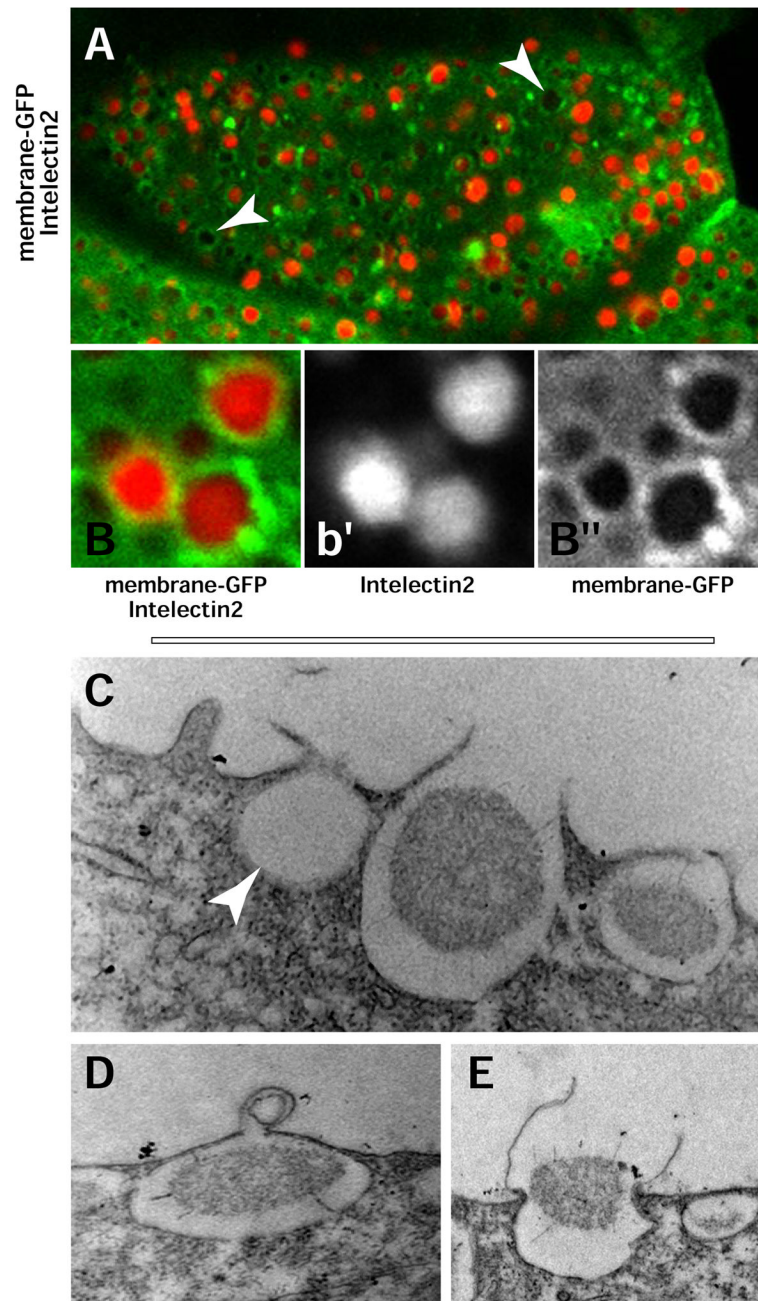
Figure 4. Goblet cells in the Xenopus epidermis secrete Intelectin-2
A. A *Xenopus* epidermis goblet cell; membrane-GFP (green) reveals the extensive exocytic vesicles; antibody staining demonstrates the presence of intelectin-2 (red) in these vesicles. Arrows mark vesicles absent of intelectin-2. **B–B".** High-magnification of exocytic vesicles shown in A. **C–E.** Transmission electron microscopy of a *Xenopus* epidermis goblet cell. **C.** Three apically-located vesicles at different stages of exocytosis are visible in an epidermal goblet cell. A mucus granule can be seen in the process of being secreted. **D.** Membrane fusion intermediate during exocytosis. **E.** Exocytic release.
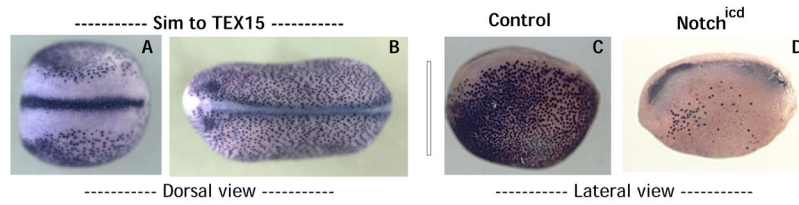
Figure 5. TEX15, a ciliated cell marker is expressed in presumptive ciliated cells and other ciliated tissues and is negatively regulated early on by Notch
TEX15 is expressed in ciliated tissues such as the midline **(A)** and the future ear **(B)**. Expression in presumptive ciliated cells in early development **(C)** is severely reduced by Notch[icd] **(D)**.
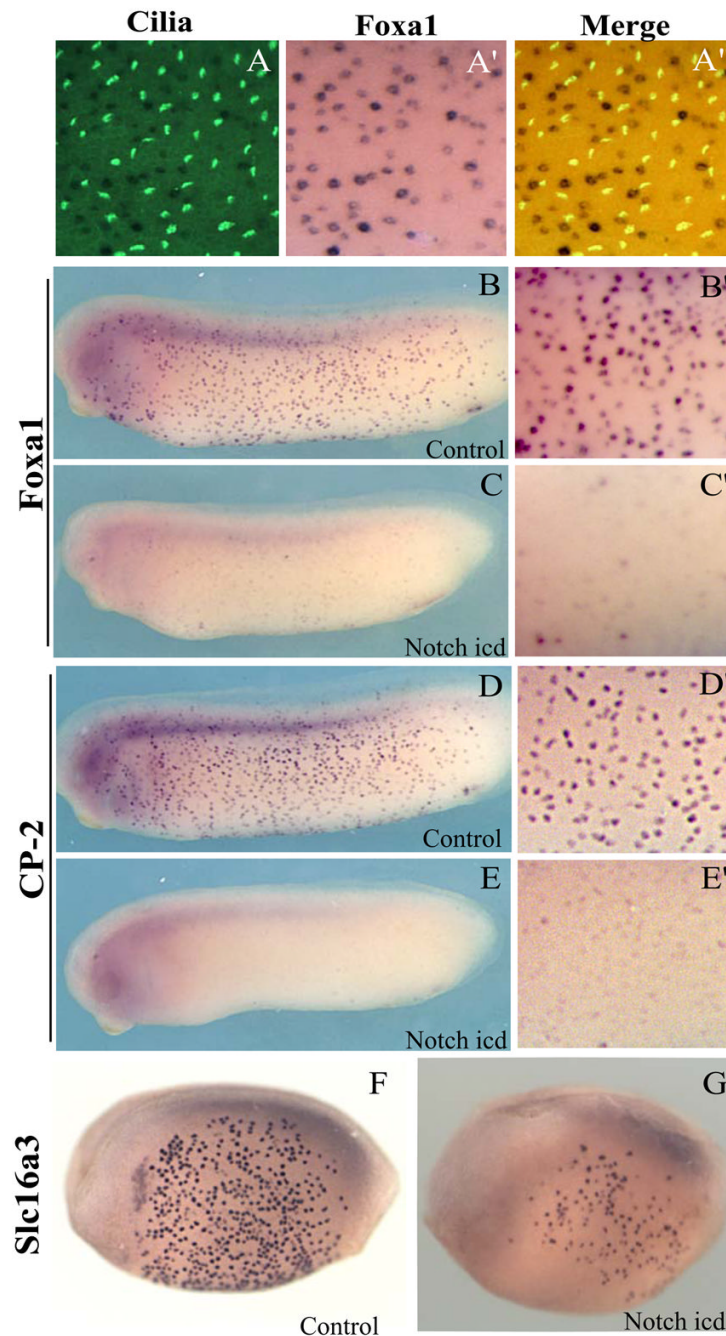
Figure 6. Small, scattered cells are negatively regulated by Notch
In situs show that genes expressed in scattered cells do not colocalize with cilia (**A–A".**).
Foxa1 and CP2 are expressed throughout the embryo at tadpole stages (**B, D**). The uneven
distribution of the cells is seen at higher magnification (**B', D'**). Injection of Notch[icd] reduces
expression of scattered cell markers in Foxa1 (**C, C'**) and CP2 (**E, E'**). Slc16a3 marks scattered
cells early in development (**F**) and its expression is also reduced by Notch[icd] (**G**).
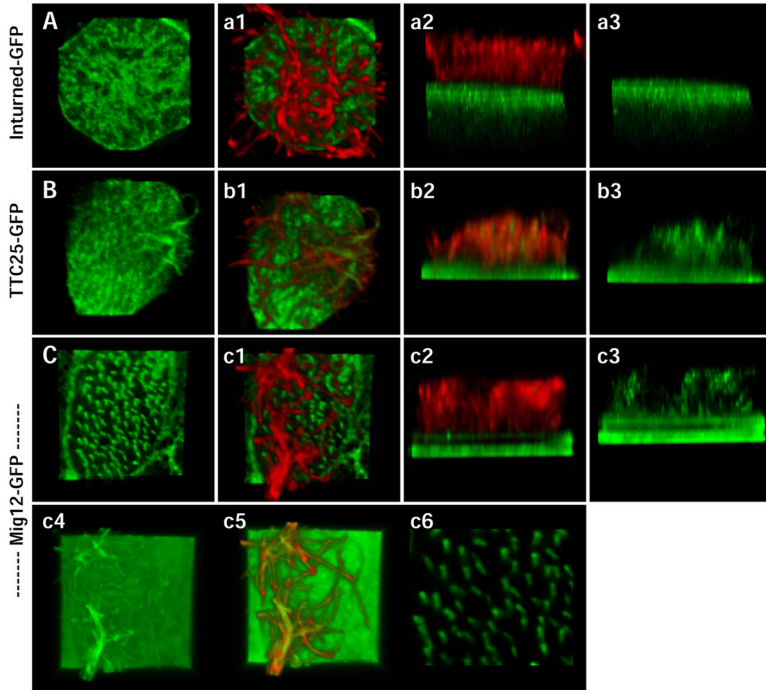
Figure 7. Mig12 and TTC25 localize to basal bodies and ciliary axoneme
Inturned-GFP, shown here as a reference, is localized at the apical surface of the ciliated cell, but is not in the ciliary axoneme **(A-a3)**. TTC25-GFP localizes to apical foci, presumably basal bodies, and also to the ciliary axoneme **(B-b3)**. Mig12-GFP localizes to both basal bodies and the ciliary axoneme **(C-c3)**. At normal gain levels, Mig12-GFP localizes very specifically to the basal bodies **(C)**, clearly marking basal body orientation and ciliary polarity **(c6)**. At high gain levels, the presence of Mig12-GFP in the ciliary axoneme is more apparent **(c4 –c5)**.
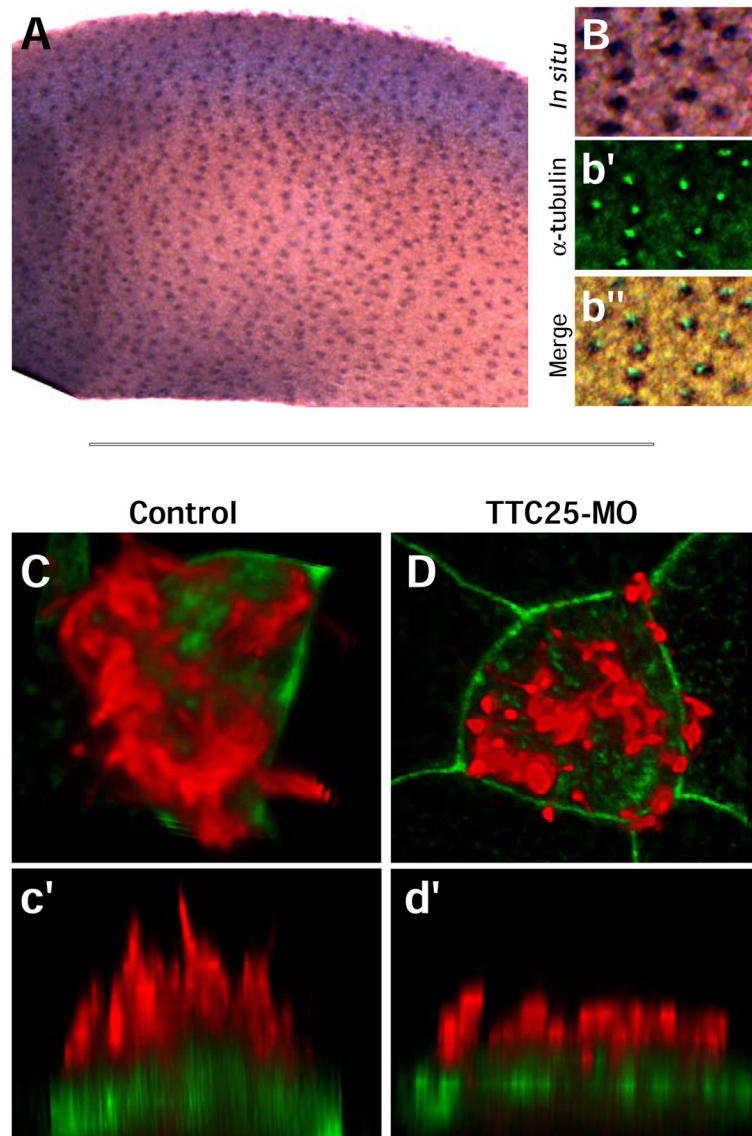
Figure 8. TTC25 is required for ciliogenesis
A. TTC25 is expressed in the evenly distributed pattern of ciliated cells, and colocalizes with cilia (**B–b"**). **C.** Ciliated cells in normal embryos develop dozens of long, thin cilia (red, anti-α-tubulin staining). **c'.** Side view of cell shown in panel A. **D,d'.** Ciliated cells in embryos injected with TTC25 MO develop only short, fat cilia. Such diminutive cilia have also been observed in embryos mutant for IFT proteins (Huangfu and Anderson, 2005).
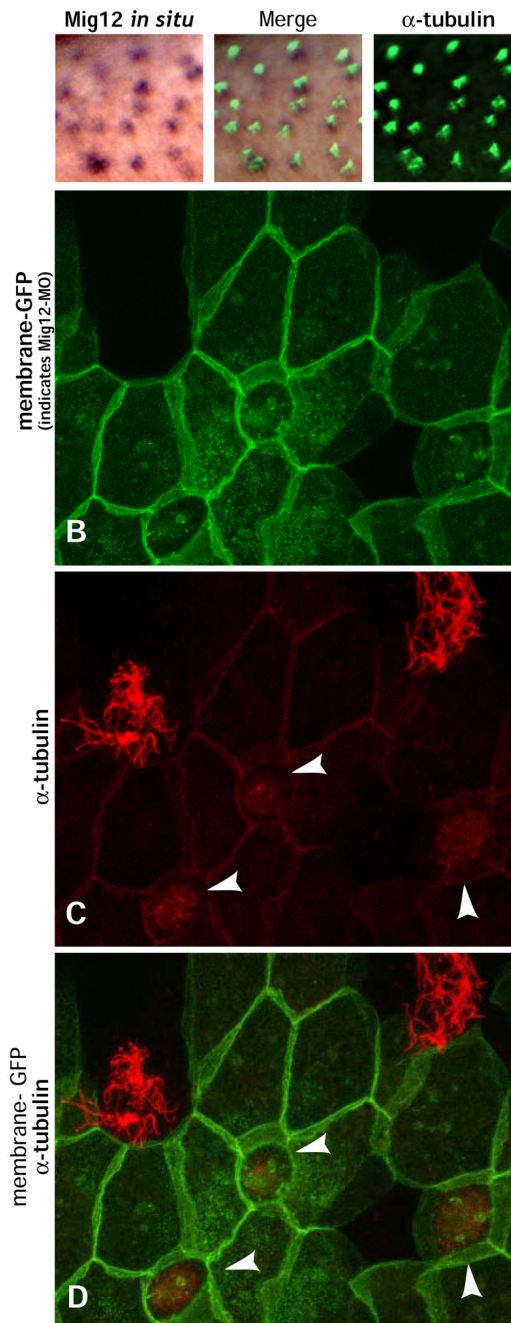
Figure 9. Mig12 is required for ciliogenesis
A–a". Mig12 *in situ* shows expression in the evenly distributed pattern of ciliated cells and colocalizes with cilia. **B–D.** Mosaic epidermis was generated by targeted co-injection of Mig12-MO and membrane-GFP. GFP-positive cells containing the MO fail to develop cilia (arrowheads). Neighboring GFP-negative cells do not contain MO and exhibit prominent tufts of large, normal cilia.
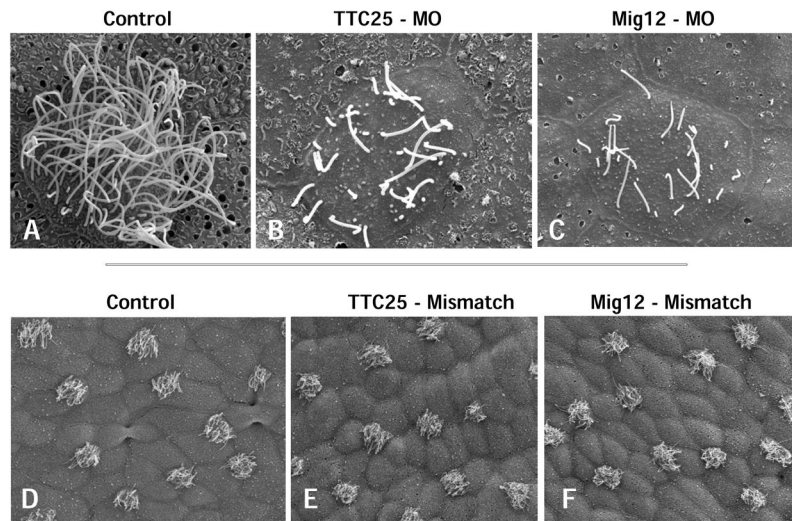
Figure 10. SEM confirms suppression of ciliogenesis in Mig12 and TTC25 morphants
A. High magnification view of a control cell shows multiple, long cilia on the apical cell surface. **B–C.** TTC25 morphants and Mig12 morphants both exhibit fewer, shortened apical cilia. **D–F.** 5-base pair mismatch morpholinos for TTC25 and Mig12 exhibit no ciliogenesis defects.

Figure 11. Novel ciliogenesis factors are required in the midline for neural tube closure
A & D. Dorsal view of TTC25 and Mig12 *in situ* shows expression in the ventral midline of the neural plate during neural tube closure. Dorsal view of an embryo injected with TTC25-MO (**B**) or Mig12-MO (**D**) both displaying a severe neural tube closure defect

Table 1

Genes previously identified as differentially-expressed in Xenopus ciliated epidermal cells
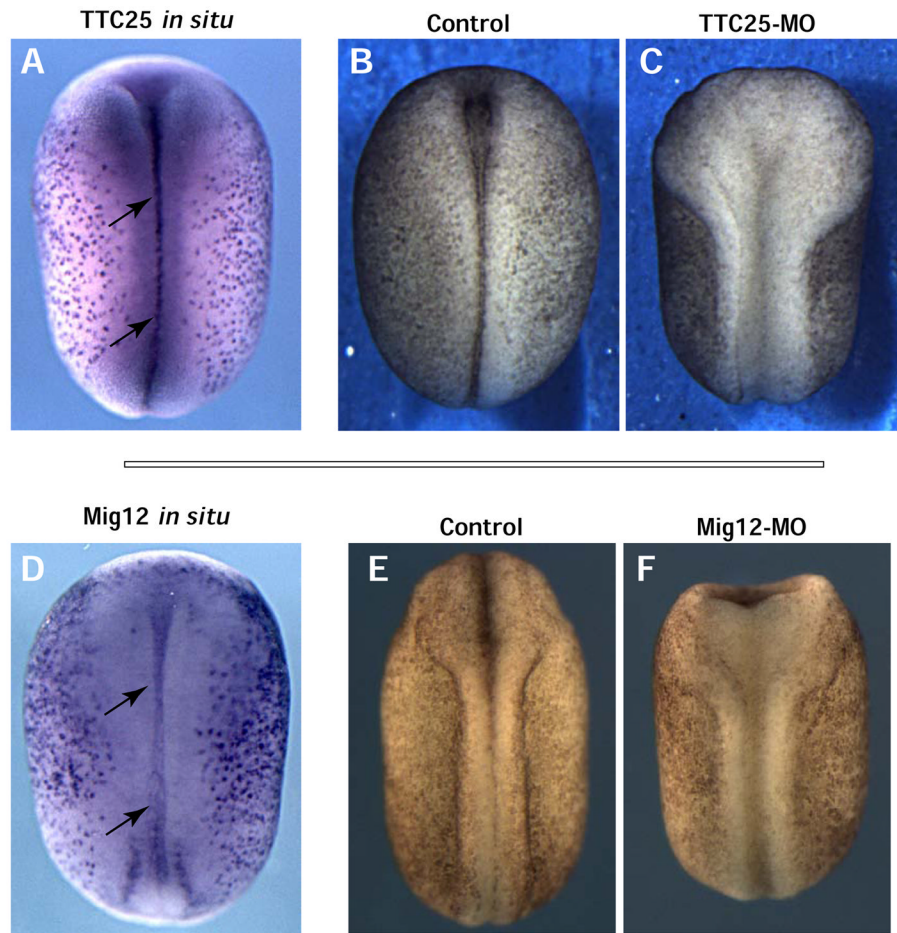
Left Column: names of genes known previously to be expressed specifically in ciliated cell of the *Xenopus* epidermis. Right Column: References

Genes	References
Cytokeleton-Related	
Fuzzy	(Park et al., 2006c)
Alpha -tubulin	(Deblandre et al., 1999)
Dynein, axonemal lig ht polypeptide 4	Pollet et al., 2005
Inner dynein arm light chain, axonemal	Pollet et al., 2005
Alpha -tubulin	Pollet et al., 2005
Beta-tubu lin	Pollet et al., 2005
Cell-fate Specification	
FoxJ1	(Pohl and Knochel, 2004)
Delta-1	(Deblandre et al., 1999)
Sox-7	Pollet et al., 2005
Other	
Caveolin-3	(Razani et al., 2002)
TRPN1	(Shin et al., 2005)
SPARC	(Huynh et al., 2000)
TTC -30	(Altmann et al., 2001)
Glutathione transferase omega -1	Pollet et al., 2005
ES-1	(Pollet et al., 2005)
FLJ3 0982	Pollet et al., 2005
ribose-phsophate pyrophosphokinase II	Pollet et al., 2005
High -affinity cGMP -specific 3′,5′ cyclic phosphodiesterase 9a	Pollet et al., 2005
Protein-tyrosine phospha tse, non-receptor type 6	Pollet et al., 2005

Table 2

Genes found to be expressed in goblet cells

Left Column: NIBB clone identifiers for individual ESTs (See Supplemental Table 1 for a hyperlinked list of genes identified in this screen, or the NIBB identifier from this table can be typed into pubmed to retrieve full sequence information for each EST). Right column, Human Orthologue or each EST.

NIBB identifier	Human Orthologue
XL084n05	Adaptor-related protein complex 2, alpha 1 subunit
XL100b06	Archain 1
XL019n06	RAB11A, member RAS oncogene family
XL049b17	RAB18, member RAS oncogene family
XL100d21	RAB28, member RAS oncogene family
XL038d18	RAB6A, member RAS oncogene family
XL005k21	Distal-less homeobox 3
XL182m22	GATA binding protein 4
XL089k19	Hairy and enhancer of split 1, (Drosophila)
XL020e14	Intelectin 2
XL010e13	Otogelin
XL017k15	Lectin
XL106l17	Mitogen-activated protein kinase 12
XL079j03	Chromosome 7 open reading frame 28A
XL088a05	Calpain 2, (m/II) large subunit
XL058a04	Caveolin 1, caveolae protein, 22kDa
XL184f23	Cyclin A1
XL014o22	6-phosphogluconolactonase
XL048a19	DnaJ (Hsp40) homolog, subfamily A, member 1
XL003n15	ELOVL family member 7, elongation of long chain fatty acids (yeast)
XL011c14	ELOVL family member 7, elongation of long chain fatty acids (yeast)
XL056f09	Fc fragment of IgG binding protein
XL091g12	Flotillin 2
XL191k21	Similar to RAS related protein 1b
XL034k20	Retinal pigment epithelium-specific protein 65kDa
XL146h03	TAF7-like RNA polymerase II
XL211g03	Thyrotrophic embryonic factor
XL094h22	TEA domain family member 1 (SV40 transcriptional enhancer factor)
XL081c06	Transcription factor CP2
XL069i11	Transcription factor CP2-like 1
XL011a05	Tripartite motif-containing 29
XL086p04	UDP-N-acteylglucosamine pyrophosphorylase 1
XL098c03	Nuclear receptor subfamily 2, group F, member 2
XL022p19	Protease, serine 27
XL089i17	Polymerase I and transcript release factor
XL079d22	KIAA1155 protein
XL076k16	Lysosomal-associated protein transmembrane 4 alpha
XL093o22	X-prolyl aminopeptidase (aminopeptidase P) 3, putative
XL105d01	No similarity
XL089i17	Polymerase I and transcript release factor
XL034h10	Vaccinia related kinase 2

Table 3

Genes found to be expressed in ciliated cells

Left Column: NIBB clone identifiers for individual ESTs (See Supplemental Table 1 for a hyperlinked list of genes identified in this screen, or the NIBB identifier from this table can be typed into pubmed to retrieve full sequence information for each EST). Right column, Human Orthologue or each EST.

NIBB identifier	Human Orthologue
XL032p09	Centrin, EF-hand protein, 2
XL048g12	Ciliary rootlet coiled-coil, rootletin
XL181e23	Tektin 3
XL082k23	Outer dense fiber of sperm tails 3
XL036o14	Outer dense fiber of sperm tails 2
XL033p01	Tubulin, beta 3
XL033o04	Interleukin 17 receptor A
XL106j22	Muscle RAS oncogene homolog
XL082i23	RAS-like, family 11, member A
XL036p21	Tetratricopeptide repeat domain 25
XL107e11	Coiled-coil domain containing 11
XL098p07	Doublecortin domain containing 2
XL034l16	MID1 interacting protein 1 (Mig12)
XL038f24	Mediator of RNA polymerase II transcription, subunit 12 homolog
XL098h16	Calcium/calmodulin-dependent serine protein kinase (MAGUK family)
XL041l02	Peroxisome proliferator-activated receptor gamma, coactivator 1 beta
XL026f02	WD repeat and SOCS box-containing 2
XL036j02	Centrosomal protein 57kDa
XL105j10	Cancer susceptibility candidate 1
XL038m18	Nucleolar protein 8
XL034l23	Cytochrome P450, family 27, subfamily B, polypeptide 1
XL036h22	Dehydrogenase/reductase (SDR family) member 7
XL105f11	Genethonin 1
XL039g17	Glyoxalase I
XL151i18	Chromosome 16 open reading frame 80
XL036i10	Nucleolar complex associated 4 homolog (S. cerevisiae)
XL082l06	PERQ amino acid rich, with GYF domain 1
XL082m16	Surfeit 2
XL102h18	Coiled-coil domain containing 19
XL009p16	Similarity to TEX15
XL038e11	THUMP domain containing 3
XL106i10	Testis specific A2 homolog (mouse)
XL065b22	Upstream transcription factor 1
XL036p06	Vesicle transport through interaction with t-SNAREs homolog 1A
XL010c09	No similarity
XL106j21	Microtubule-associated protein 1 light chain 3 gamma
XL082o19	Coiled-coil domain containing 78, isoform 1

Table 4

Genes found to be expressed in small, scattered cells

Left Column: NIBB clone identifiers for individual ESTs (See Supplemental Table 1 for a hyperlinked list of genes identified in this screen, or the NIBB identifier from this table can be typed into pubmed to retrieve full sequence information for each EST). Right column, Human Orthologue or each EST.

NIBB identifier	Human Orthologue
XL175g13	Core-binding factor, runt domain, alpha subunit 2; translocated to, 2
XL009f10	Carbohydrate (N-acetylgalactosamine 4–0) sulfotransferase 9
XL180m23	E2F transcription factor 3
XL019o09	zinc finger protein 750
XL084c06	Forkhead box A1
XL016g24	Forkhead box I1
XL048b04	Forkhead box I1
XL031e11	Growth differentiation factor 8
XL071b24	scribbled homolog
XL033k03	Membrane-associated ring finger (C3HC4) 5
XL003a10	No similarity
XL049e23	RAP2B, member of RAS oncogene family
XL180m22	Runt-related transcription factor 1; translocated to, 1 (cyclin D-related)
XL010k16	Sarcoglycan, epsilon
XL041n11	Serum/glucocorticoid regulated kinase
XL013d10	Solute carrier family 16 (monocarboxylic acid transporters), member 3
XL017m18	SRY (sex determining region Y)-box 11
XL143p23	upstream binding protein 1 (LBP-1a)
XL170d08	X-box binding protein 1
XL022d15	No similarity
XL026g21	zinc finger, AN1-type domain 5
XL013m12	Smoothelin
XL020n06	No similarity
XL021g20	No similarity
XL047b23	No similarity
XL196l23	No similarity